25th ABCM International Congress of Mechanical Engineering
October 20-25, 2019, Uberlândia, MG, Brazil

COB-2019-0186
A CASE STUDY IN ENERGY CONSUMPTION ESTIMATES FOR ELECTRIC AIRCRAFT MISSION PLANNING

Guilherme N. Barufaldi
Mauricio A. V. Morales
Roberto Gil A. da Silva
Instituto Tecnológico de Aeronáutica, Praça Mal. Eduardo Gomes, 50, Vila das Acácias, CEP: 12228-900, São José dos Campos - SP - Brazil
guilherme.barufaldi@protonmail.com, morales@ita.br, gil@ita.br

Abstract. *In recent years, electric airplanes have become a topic of great interest for the aeronautical community. From small unmanned aerial vehicles to manned light sporting aircraft, this emerging segment is quickly gaining space in the aviation market. However, the study of electric aircraft performance is still being established. Since the propulsion system is different from internal combustion engines, performance characteristics and operational issues can differ significantly from that of regular aircraft. These particular aspects must be taken into account when preparing the operation. In this paper, procedures for obtaining estimates of electrical energy consumption for mission and flight planning are presented. These estimates are critical to assess mission feasibility, safety margins, costs, etc. The method is based on approximate, analytical solutions, allowing quick calculations, which is convenient for the task, and can also be employed during the conceptual design phase.*

Keywords: *Electric aircraft, flight performance, aircraft operation, flight planning, aircraft conceptual design*

1. INTRODUCTION

Electric propulsion has arisen as a possible solution to aviation pollution and noise problems, since electric motors can function with nearly zero emissions *in situ*, and low noise levels. This type of propulsion usually consists of propellers or ducted fans driven by electric motors. Its development started during the 1950s, initially with small model aircraft and UAVs, and more recently with motor gliders and light sporting aircraft (LSA).

The emerging market for manned electric aircraft is currently comprised of personal sporting airplanes and gliders, such as the Taurus Electro (Pipistrel, 2007) or the Arcus-e (Schempp-Hirth, 2012). However, light electric training aircraft are expected to become operational and occupy a market share in the near future, due to the rising cost of aviation fuel (Moore and Fredericks, 2014). With more and more restrictions being imposed on pollutant emissions and noise, leading aircraft manufacturers and research institutions are also turning their attention to the development of electric and high-efficiency airplanes – so called “green aircraft”.

Boeing Co. has funded the development of a hybrid-electric airplane (Boeing, 2015). Airbus Group has developed the all-electric E-Fan and is currently involved in the design of the new hybrid-electric E-Fan X (Airbus, 2018). NASA has been researching electric aircraft and distributed propulsion (NASA, 2017), and the German Aerospace Center (DLR) has successfully developed and flown the HY4, powered solely by a hydrogen fuel cell system (DLR, 2016). In academia, there is significant effort to improve electric propulsion technologies, and also to understand how it affects the overall aircraft performance.

Among important works, Hepperle (2012) studied range capabilities and limitations imposed by current battery technology. Sachs (2012) showed that the performance of an all-electric aircraft differs significantly of a comparable vehicle with air-breathing propulsion. Traub (2011) analyzed the impact of the Peukert effect on the range and endurance of electric aircraft powered by batteries, and provided ways for estimating those performance characteristics. Furthermore, since electric aviation is a relatively new field, the performance models are still being established.

In this paper, an analytical method to obtain estimates of electrical energy consumption for mission and flight planning is presented, with a case study involving an electric motor glider currently under development. Obtaining these estimates is a standard procedure in aviation, since they are critical to assess mission feasibility, safety margins, costs and estimated times for flight scheduling. The energy approach is useful for comparing the performance of electric aircraft with those equipped with internal combustion engines (ICEs), as well as for estimating battery or fuel cell mass during the conceptual design phase. It is also useful for obtaining mission cost estimates due to electric energy consumption.

2. METHOD

The proposed method is based on approximate analytical solutions to calculate electrical energy consumption estimates. These solutions allow quick computations, which is convenient for the task of mission planning, and for the conceptual design phase of an electric aircraft. Since the goal is estimating energy consumption, and not directly controlling the plant, there is no need to deal with the dynamic model based on differential equations.

2.1 Aircraft and propulsion models

The aerodynamic force acting on the aircraft can be broken down in two components, the lift L and the drag D, such that:

$$L = \frac{\rho V^2}{2} S C_L \tag{1}$$

$$D = \frac{\rho V^2}{2} S C_D \tag{2}$$

where ρ is the air density; V is the aircraft velocity; S is the wing reference area; and C_L is the dimensionless lift coefficient. C_D is the dimensionless drag coefficient, and can be modelled as a quadratic function of C_L, as show by Eq. (3), where C_{D_0} is the zero lift drag coefficient, and k is the lift-dependent drag constant.

$$C_D = C_{D_0} + k C_L^2 \tag{3}$$

The propulsion system of a propeller-driven, electric aircraft can be modeled by the following equations (Sachs, 2012):

$$P_{\text{el}} = P_{\text{el}}^{\text{max}} \delta_m \tag{4}$$

$$T = \frac{\eta P_{\text{el}}^{\text{max}}}{V} \delta_m \tag{5}$$

Equation (4) states that the motor electric power P_{el} is proportional to the normalized throttle opening δ_m ($0 \leq \delta_m \leq 1$), controlled by the pilot. Hence, the pilot selects a fraction of the maximum electric power $P_{\text{el}}^{\text{max}}$ by defining the input δ_m. Equation (5) states that the available thrust force T is proportional to δ_m and a total efficiency coefficient η, and inversely proportional to the aircraft velocity V.

The coefficient η combines the efficiency of all elements in the propulsion system, especially the motor and propeller efficiencies. It varies with the aircraft velocity V and the propeller rotational speed Ω, with both values V and Ω being usually described in the aircraft operation manual. For conceptual design purposes, the propeller efficiency η_{pr} values for each flight phase can be found in references such as (Torenbeek, 1982) or (Stickle and Crigler, 1941). The motor efficiency should be provided by the manufacturer, but if data is not available, or the motor has not yet been defined, its efficiency η_{m} can be assumed to be some value between 0.85 and 0.95 (modern DC brushless electric motors can achieve efficiencies of up to 98%). The total efficiency can be calculated from Eq. 6.

$$\eta = \eta_{\text{pr}} \cdot \eta_{\text{m}} \tag{6}$$

Many calculations use the stall speed V_{s} as a parameter, as shown by Eq. (7):

$$V_{\text{s}} = \sqrt{\frac{2W}{\rho S C_{L_{\text{max}}}}} \tag{7}$$

where W is the aircraft weight and $C_{L_{\text{max}}}$ is the maximum lift coefficient. V_{s} is the minimum velocity that an aircraft can keep when in leveled flight, and it is reached when the lift coefficient C_L is at its maximum value, $C_{L_{\text{max}}}$. It should be noted that V_{s} changes with aircraft weight, altitude (because ρ decreases with increasing altitude) and $C_{L_{\text{max}}}$, which can be increased with flap deflection.

2.2 Ground roll and takeoff

The ground roll phase is predominantly transient, especially for a propeller driven airplane. The aircraft accelerates from zero velocity until reaching the liftoff speed V_{LO}, when the main landing gear loses contact with the ground. During this phase, the acceleration with respect to the ground a_{gr} is:

$$a_{\text{gr}} = \frac{g}{W}\left[T - D - \mu(W - L)\right] \tag{8}$$

where g is the acceleration of gravity; μ is the friction coefficient between the aircraft and the ground. Despite the presence of non-stationary phenomena, a reasonable approximation can be obtained by considering the term $[T - D - \mu(W - L)]$ constant and equal to its value when $V = 0.7V_{\text{LO}}$ (Anderson, 1999). Considering this approximation, the ground roll distance s_{gr} for a small aircraft is:

$$s_{\text{gr}} = V_{\text{LO}}\left\{\frac{WV_{\text{LO}}}{2g}\left[\frac{1}{T - D - \mu(W - L)}\right] + 1\right\} \tag{9}$$

Since the acceleration a_{gr} is assumed constant, then the ground roll time Δt_{gr} is:

$$\Delta t_{\text{gr}} = \sqrt{\frac{2s_{\text{gr}}}{a_{\text{gr}}}} \tag{10}$$

During the ground roll, takeoff, and the initial climb phase, the normal procedure requires the pilot to keep the power at maximum value, i.e., $\delta_m = 1$ (FAA, 2018). Therefore, the electrical energy spent during the ground roll phase E_{gr} can be obtained by multiplying Eq. (4) by the result of Eq. (10):

$$E_{\text{gr}} = P_{\text{el}}^{\text{max}} \cdot \Delta t_{\text{gr}} \tag{11}$$

The liftoff speed V_{LO} is given by the manufacturer in the aircraft operation manual. If the calculations are being made for the conceptual design, the liftoff speed can be estimated as $V_{\text{LO}} = 1.15V_{\text{s}}$, with V_{s} corresponding to the flap deflection being used for take-off. The drag force D in Eqs. (8) and (9) must be calculated by taking into account the ground effect and drag increase due to flap deflection and landing gear extension. In this case, a modification of Eq. (3) can be used (Anderson, 1999):

$$C_D = C_{D_0} + \Delta C_{D_0} + k' C_L^2 \tag{12}$$

The zero lift drag increase ΔC_{D_0} can be estimated according to Eq. (13), where m_{max} is the aircraft maximum mass, in kilograms, and K_{uc} is a constant such that $K_{\text{uc}} = 5.81 \times 10^{-5}$ for zero flap deflection, and $K_{\text{uc}} = 3.16 \times 10^{-5}$ for full flap deflection – intermediate cases can be found through linear interpolation.

$$\Delta C_{D_0} = \frac{W}{S} \cdot K_{\text{uc}} \cdot m_{\text{max}}^{-0.215} \tag{13}$$

The modified lift-dependent drag constant k' can be estimated according to Eq. (14), where k_1 is the term related to the viscous drag, h is the average height of the wing above the ground, b is the wingspan, e is the wing Oswald factor, and AR is the wing aspect ratio. Methods for estimating k_1, or the other parameters during conceptual design can be found in references such as (Raymer, 2006) or (Torenbeek, 1982).

$$k' = k_1 + \frac{(16h/b)^2}{1 + (16h/b)^2} \cdot \frac{1}{\pi \cdot e \cdot AR} \tag{14}$$

2.3 Climb

For calculation purposes, we consider that the climb phase begins soon after lift off, i.e., after the main landing gear loses contact with the ground, and lasts until the aircraft reaches the cruise altitude – for safety purposes though, regulations state that the climb phase begins after the aircraft has cleared a minimum height of 35 ft. Since the transient effects are less pronounced, the steady state approximation yields good results (Anderson, 1999). During this phase, the normal procedure in general aviation is to use the elevator control (stick) to regulate velocity and the throttle control to

regulate the rate of climb (FAA, 2018). The climb velocity V_{cl} can also be defined in function of the stall speed, and is usually recommended in the aircraft manual. The climb performance of an electric aircraft is discussed in more detail in (Barufaldi *et al.*, 2019), where an expression for the energy spent during climb E_{cl} as a function of C_L and δ_m was formulated, as shown here in Eq. (15):

$$E_{\text{cl}} = \frac{P_{\text{el}}^{\max}\delta_m \Delta h}{\frac{\eta P_{\text{el}}^{\max}}{W}\delta_m - \sqrt{\frac{2WC_{D_0}^2}{\rho S}}C_{L_{\text{cl}}}^{-3/2} - \sqrt{\frac{2Wk^2}{\rho S}}C_{L_{\text{cl}}}^{1/2}} \tag{15}$$

In Eq. (15) the air density value is the average between the surface and the cruise altitude values. The lift coefficient during the climb phase can be found according to Eq. (16):

$$C_{L_{\text{cl}}} = \frac{2W}{\rho S V_{\text{cl}}^2} \tag{16}$$

The climb begins with full power ($\delta_m = 1$) until a certain height, usually 500 ft in general aviation, and then the pilot sets the throttle back to approximately 85% ($\delta_m = 0.85$), depending on the aircraft weight, air density and the desired rate of climb (RoC). The climb speed V_{cl} is given by the manufacturer in the aircraft operation manual, or can be estimated as $V_{\text{cl}} = 1.2V_{\text{s}}$.

2.4 Cruise

During cruise, the aircraft keeps leveled flight, maintaining a desired altitude, for which the air density value is ρ_{cr}. The cruise velocity V_{cr} can be selected in function of the mission goals, such as minimum time, maximum range, or could be imposed by air traffic control (ATC). In any case, the cruise velocity will determine the value of C_L because of the relation $L = W$, that is, weight equals lift:

$$C_{L_{\text{cr}}} = \frac{2W}{\rho_{\text{cr}} S V_{\text{cr}}^2} \tag{17}$$

In this equilibrium condition, drag equals thrust. From Eqs. (5) and (2), $T = D$ yields:

$$\delta_{m_{\text{cr}}} = \frac{\rho_{\text{cr}} V_{\text{cr}}^3 S C_{D_{\text{cr}}}}{2\eta P_{\text{el}}^{\max}} \tag{18}$$

Equation (18) gives the necessary throttle opening to trim the aircraft in cruise flight, for a given altitude and velocity. $C_{D_{\text{cr}}}$ is the drag coefficient for cruise, obtained by substituting the result of Eq. (17) into Eq. (3). The cruise time Δt_{cr} can be found from Eq. (19):

$$\Delta t_{\text{cr}} = \frac{s_{\text{cr}}}{V_{\text{cr}}} \tag{19}$$

where s_{cr} is the distance to be traveled while in cruise, obtained from navigation calculations. Finally, the total electrical energy spent during cruise phase E_{cr} can be calculated as shown in Eq. (20):

$$E_{\text{cr}} = P_{\text{el}}^{\max} \cdot \delta_{m_{\text{cr}}} \cdot \Delta t_{\text{cr}} \tag{20}$$

The velocity for maximum range is attained for the lift coefficient C_L^*, shown in Eq. (21) (Kaptsov and Rodrigues, 2018):

$$C_L^* = \sqrt{\frac{C_{D_0}}{k}} \tag{21}$$

2.5 Loiter

A loiter phase takes place if the aircraft needs to overfly an area, for a specific mission or to wait for ATC clearance. The aircraft usually follows a smooth flight pattern, such that it can be considered as leveled steady flight, maintaining a desired altitude, for which the air density value is ρ_{ltr}. The loiter velocity V_{ltr} can be selected in function of the mission goals, such as maximum endurance, or be imposed by ATC. In any case, the loiter velocity will determine the value of C_L because of the relation $L = W$.

The lift coefficient during loiter $C_{L_{\text{ltr}}}$ can be obtained from Eq. (17) with V_{ltr}, and the throttle opening $\delta_{m_{\text{ltr}}}$ can be obtained from Eq. (18), with loiter data. Finally, the total electrical energy spent during loiter E_{ltr} can be obtained with

Eq. (20), by using loiter data – the loiter time Δt_{ltr} is specified by the mission planner or ATC. In case the aircraft is not restricted by mission velocity requirements or ATC, the lift coefficient for maximum endurance can be obtained from Eq. (22) (Kaptsov and Rodrigues, 2018):

$$C_{L_{\text{ltr}}} = \sqrt{\frac{3C_{D_0}}{k}} \tag{22}$$

2.6 Descent

The descent phase occurs whenever the aircraft needs to decrease its altitude, either to change flight level or to prepare to land at its destination. It can happen continuously or in several steps. Whichever way, the pilot adjusts the airspeed by controlling the attitude of the aircraft and regulates the rate of descent by adjusting the throttle opening. For most small propeller-driven airplanes, descents are conducted by setting the throttle to idle position, in such a way that the thrust produced by the propeller can be neglected. In this case, the descent slope can be calculated according to Eq. (23):

$$|\gamma| \approx \frac{C_D}{C_L} \tag{23}$$

Thus, the vertical velocity, or rate of descent can be calculated as shown in Eq. (24):

$$V_z \approx V_{\text{des}} \left(\frac{1}{L/D} \right) \tag{24}$$

where the parameter L/D is the glide ratio (aerodynamic efficiency) at this condition, and V_{des} is the velocity during descent, usually stated in the aircraft manual. For small airplanes or motor gliders, the descent velocity is equal or relatively close to cruise speed, and could be estimated to being equal to the best power-off glide speed, obtained from $T = D$, with $C_L = C_L^*$, the value shown in Eq. (21). It is worth noting that the glide ratio and the velocity depend on each other. Therefore, the time to descend an altitude variation Δh can be calculated according to Eq. (25):

$$\Delta t_{\text{des}} = \frac{\Delta h}{V_{\text{des}}} \left(\frac{L}{D} \right)_{\text{des}} \tag{25}$$

Finally, the electric energy spent during descent is obtained from Eq.

$$E_{\text{des}} = P_{\text{el}}^{\text{max}} \cdot \delta_{m_{\text{des}}} \cdot \Delta t_{\text{des}} \tag{26}$$

where $\delta_{m_{\text{des}}}$ is the throttle opening to be kept during the descent phase – usually the idle position, described in the aircraft or the motor manual. However, since electric motors can be easily shut down and restarted, the descent phase can be conducted with no power whatsoever, that is, $\delta_{m_{\text{des}}} = 0$, in order to save energy. The electric energy spent during landing can be neglected, since landing time is small, and the throttle is usually kept at idle or a low value.

3. RESULTS AND DISCUSSION

3.1 Aircraft parameters

The aircraft model of the CENIC C-1 (Fig. 1) will be used to exemplify the method and provide a quantitative insight to it. It is an all-composite electric motor glider being developed at CENIC Engineering, a company located in São José dos Campos, Brazil, and features a Enstroj EMRAX brushless DC motor, with a folding carbon fiber propeller, custom-made by Electravia in France. The motor is powered by lithium-polymer batteries. Relevant parameters are shown in Table 1 [1].

3.2 Case study: air taxi flight

An air taxi flight is defined as is a short flight made on demand by small commercial aircraft. A typical air taxi flight profile is illustrated in Fig. 2: the aircraft rolls, takes off, climbs until cruising altitude, travels along its route, then descends and lands. This flight profile is a simple example of a light transportation mission or an aircraft transference from one aerodrome to another, and it does not incorporate eventual altitude changes required by ATC.

Figure 1. C-1, an electric motor glider currently being developed at CENIC Engineering, in São José dos Campos, Brazil.

Table 1. CENIC C-1 motor glider relevant technical data.

Parameter	Value	Unit
Wing span (b)	15	m
Wing area (S)	12.5	m^2
Wing aspect ratio (AR)	18	–
Max. take-off mass (m_{max})	430	kg
Zero-lift drag coefficient (C_{D_0})	0.011	–
Lift-dependent drag constant (k)	0.021	–
Motor maximum electric power ($P_{\text{el}}^{\text{max}}$)	30	kW
Stall speed at sea level (for m_{max})	70	km/h
Maximum glide ratio (max. $^L/_D$)	32.9	–

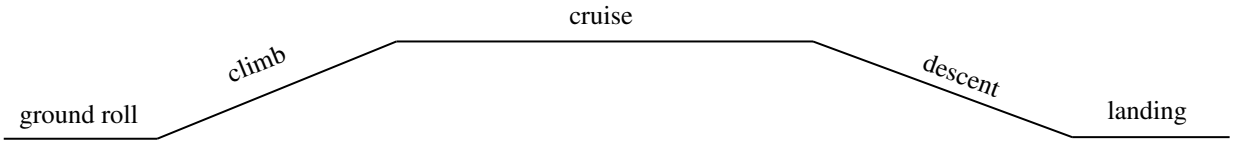

Figure 2. Air taxi flight typical profile.

The mission starts with the aircraft described in Sec. 3.1 taking off from a regular paved runway, for which the friction coefficient is $\mu = 0.04$ (Raymer, 2006), at sea level. The ground roll initiates with full power ($\delta_m = 1$) and proceeds until take-off, that is, the moment that the lift-off speed (V_{LO}) is reached. The climb phase is assumed to start shortly thereafter, with 85% of the maximum power ($\delta_m = 0.85$). The aircraft then climbs until reaching an altitude of 4000 ft.

The cruise phase takes place after the desired altitude is reached. The airspeed is 110 km/h, and it is maintained throughout the course of 50 km. The vertical of the destination aerodrome is located at the final point of the cruise leg. The airplane then starts a smooth, descending spiral, until final approach and landing. For the sake of simplicity, the descent is assumed to end at the runway level, and the energy spent during landing is not accounted for, such as described in Sec. 2.6. During this last phase, the aircraft maintains an airspeed of 90 km/h, and the throttle is kept at idle.

The calculations employ the formulas presented in Sec. 2., and the results are shown in Table 2. The total flight time is approximately 57 minutes, which is within the limits of the C-1 batteries. The total electric energy spent during flight is 7.8 kWh. It is worth noting that the energy consumed to climb 4000 ft is very high when compared to the total, which highlights the fact that the climb phase is very demanding to the propulsion system.

The descent phase takes a long time to finish, almost as long as the cruise. This was chosen on purpose, to illustrate the fact that an aerodynamically efficient aircraft can have a high power-off glide ratio – in this case, the glide slope during descent is only -1.8°, as show in Table 2. Although not common for small general aviation aircraft, this descent pattern is usual for gliders and motor gliders. The electric motor could have been turned off, because of the aircraft's high aerodynamic efficiency, and the fact that an electric motor can easily be restarted, another advantage of this type of aircraft. One way to reduce the descent time is to use spoilers, which increase drag and considerably lower the $^L/_D$ ratio – in this case, to account for the spoiler drag, another term ΔC_{D_0} should be added in Eq. (3).

[1] Values kindly provided by the engineering team at CENIC.

Table 2. Calculation results for the air taxi flight, with the CENIC C-1 model.

Phase	Parameter	Value	Unit
Ground roll	V_{LO}	76	km/h
	a_{gr}	2.45	m/s^2
	s_{gr}	112.5	m
	$C_{L_{\text{gr}}}$	1.25	–
	Δt_{gr}	9.6	s
	E_{gr}	79.9	Wh
Climb	Δh	4000	ft
	V_{cl}	83	km/h
	$C_{L_{\text{cl}}}$	1.1	–
	Δt_{cl}	4.2	min
	E_{cl}	2.38	kWh
Cruise	s_{cr}	50	km
	V_{cr}	110	km/h
	$C_{L_{\text{cr}}}$	0.67	–
	Δt_{cr}	27.3	min
	E_{cr}	2.76	kWh
Descent	V_{des}	90	km/h
	γ	-1.8	degrees
	$C_{L_{\text{des}}}$	1	–
	Δt_{des}	25.4	min
	E_{des}	2.58	kWh

4. CONCLUSIONS

This work has presented a method based on approximate analytical solutions to calculate energy consumption estimates for electric aircraft mission planning. The method can also be employed for conceptual design estimations. The analytical expressions allow quick calculations, which is efficient and convenient. The usage of electric energy also allows engineers to estimate battery or fuel cell mass, and energy costs and its impact on total operational costs. Since the performance models of electric aircraft are still being established, the presented method could help research groups to conduct comparisons with conventional aircraft equipped with internal combustion engines. In order to exemplify the method and provide quantitative insight, calculations were made based on a real aircraft model. For future works, more detailed propulsion models could be employed, ones that include propeller data. Another suggestion for future contributions could be the inclusion of power sources particular phenomena, such as the variation of battery voltage with current draw.

5. ACKNOWLEDGEMENTS

This study was financed in part by the Coordenação de Aperfeiçoamento de Pessoal de Nível Superior – Brasil (CAPES) – Finance Code 001, under the research grant number 88882.180826/2018-01.

6. REFERENCES

Airbus, 2018. "The future is electric". Airbus Group. URL https://www.airbus.com/innovation/The-future-is-electric.html/. Retrieved 15 Feb. 2019.

Anderson, J.D., 1999. *Aircraft Performance and Design*, McGraw-Hill, New York, pp. 199–364.

Barufaldi, G.N., Morales, M.A.V. and da Silva, R.G.A., 2019. "Energy optimal climb performance of electric aircraft". In *AIAA SciTech Forum*. doi:10.2514/6.2019-0830.

Boeing, 2015. "Here's Watts Up: We've Got the Power". Boeing Company. URL http://www.boeing.com/features/2015/01/corp-hybrid-01-05-15.page. Retrieved 17 Feb. 2019.

DLR, 2016. "Zero-emission air transport: first flight of four-seat passenger aircraft HY4". Deutsches Zentrum für Luft- und Raumfahrt e.V. URL https://www.dlr.de/dlr/en/desktopdefault.aspx/tabid-10081/151_read-19469/#/gallery/24480. Retrieved 12 Feb. 2019.

FAA, 2018. *Airplane Flying Handbook*. Federal Aviation Administration Flight Standards Service, Washington DC.

Hepperle, M., 2012. "Electric flight – potential and limitations". In *Proceedings of the NATO Science and Technology*

Organization Meeting. Vol. 209.

Kaptsov, M. and Rodrigues, L., 2018. "Electric aircraft flight management systems: economy mode and maximum endurance". *Journal of Guidance, Control and Dynamics*, Vol. 41, No. 1, pp. 285–290. doi:10.2514/1.G002806.

Moore, M.D. and Fredericks, B., 2014. "Misconceptions of electric propulsion aircraft and their emergent aviation markets". In *AIAA SciTech Forum, 52nd Aerospace Sciences Meeting*. doi:10.2514/6.2014-0535.

NASA, 2017. "NASA Armstrong Fact Sheet: X-57 Maxwell". National Air and Space Administration. URL `https://www.nasa.gov/centers/armstrong/news/FactSheets/FS-109.html`. Retrieved 9 Jun. 2018.

Pipistrel, 2007. "Taurus electro motor glider". Pipistrel Aircraft. URL `https://www.pipistrel-aircraft.com/aircraft/electric-flight/taurus-electro/`. Retrieved 17 Feb. 2019.

Raymer, D.P., 2006. *Aircraft Design: A Conceptual Approach*. AIAA Education Series. AIAA American Institute of Aeronautics and Astronautics, 4th edition.

Sachs, G., 2012. "Flight performance issues of electric aircraft". In *AIAA Atmospheric Flight Mechanics Conference, Guidance, Navigation, and Control and Co-located Conferences*. doi:10.2514/6.2012-4727.

Schempp-Hirth, 2012. "The Arcus-E Sailplane". Schempp-Hirth Flugzeugbau GmbH. URL `https://www.schempp-hirth.com/en/sailplanes/arcus/arcus-e.html`.

Stickle, G.W. and Crigler, J.L., 1941. *Propeller Analysis from Experimental Data NACA-TR-712*. National Advisory Committee for Aeronautics.

Torenbeek, E., 1982. *Synthesis of Subsonic Airplane Design*. Springer, 1st edition.

Traub, L.W., 2011. "Range and endurance estimates for battery-powered aircraft". *Journal of Aircraft*, Vol. 48, No. 2, pp. 703–707. doi:10.2514/1.C031027.

7. RESPONSIBILITY NOTICE

The authors are the only responsible for the printed material included in this paper.